*Geochemistry International, Vol. 42, No. 7, 2004, pp. 630–640. Translated from Geokhimiya, No. 7, 2004, pp. 729–739.*

# Geochemistry of Sumian Basaltic Andesites of Central Karelia

**S. A. Svetov, A. I. Golubev, and A. I. Svetova**

*Institute of Geology, Russian Academy of Sciences, Karelian Research Center, Pushkinskaya ul. 11,*
*Petrozavodsk, 185610 Russia*
*e-mail: ssvetov@krc.karelia.ru*

Received June 12, 2002

**Abstract**—A large Paleoproterozoic province of rocks of basaltic andesite composition with a high magnesium content (MgO = 5–10 wt %) was formed within the Karelian craton 2.55–2.4 Ga ago. The representative Sumian sequences were described in Central Karelia near Krasnaya Rechka and Koikary villages, Semch River, and Kumsa structure. Massive, amygdaloidal, variolitic, and pillow lava flows 9–45 m thick dominate the sections with reconstructed thicknesses up to 1500–1650 m. Tuffs compose rare interbeds. Based on variations of the $SiO_2$, $TiO_2$, and MgO contents in rocks, up to seven volcanic stages can be distinguished. The volcanic rocks are similar to boninites by their concentrations of $SiO_2$ (54.62 ± 3.14 wt %), Ni (135 ± 70 ppm), Cr (295 ± 134 ppm), but significantly differ from them by Mg# (#Mg = 50.05 ± 6.22); concentrations of $TiO_2$ (0.84 ± 0.26 wt %), Hf (<4.2 ppm), Ta (<0.7 ppm), Zr (<120 ppm); and topology of REE spectra with $(La/Sm)_n$ = 1.6–5.2 and $(Ce/Yb)_n$ = 4.1–18.6. Model calculations testify to a shallow origin of initial magmas, which is typical of volcanic rocks of subduction zones. Geochemical characteristics of Sumian volcanic associations allow us to correlate them with basaltic andesites of active continental margins of the Andean type.

## INTRODUCTION

Distinguishing the “boninite-like” volcanic series in greenstone belts has been actively discussed recently. These series are revealed now in the Archean greenstone belts, such as Nondweni, South Africa [1]; Abitibi, Canada [2]; and Iringora and Hizovaara structures in Fennoscandia [3, 4]; and in the Lower Proterozoic greenstone belts and structures [5, 6], such as Vetrenyi Belt in Eastern Karelia, Pechenga, Imandra–Varzuga (Kola Peninsula), and other localities [7, 8].

In this paper the authors summarize new data on REE distribution in rocks of basaltic andesite associations from Sumian sequences of Central Karelia (the lower part of the Sumian–Sariolian sedimentary–volcanic complex is regarded as Sumian volcanic associations [9]), such as in the sections near Krasnaya Rechka and Koikary villages, along the Semch River, and in the Kumsa structure, which are representative of the large Paleoproterozoic magmatic province of the Karelian craton. Our investigation is aimed at revealing the initial geochemical features of Sumian lavas, their affinity to boninites (?), and possible geodynamic setting of their formation.

## GEOLOGICAL DESCRIPTION OF THE ASSOCIATION

We studied Sumian volcanic rocks of Central Karelia (northwestern Onega region) in the area of Kumsa structure, Krasnaya Rechka village, Semch River, and Koikary village (Fig. 1), where they form a thick sequence of interbedded lava flows with a total thickness of up to 1500–1650 m [10–15].

The Sumian volcanic association overlays the Upper Archean deposits with angular unconformity; contains at its base a zone of residual–talus breccias (Semch and Koikary structures) or a sedimentary unit of siltstones, sandstones, and tuffites 150 m thick (Kumsa structure); and lies on weathered granites near the Krasnaya Rechka village. The Sumian sequence is overlain by thick units of polymict conglomerates with interbeds of Sariolian sandstones and gritstones in all considered structures.

Lithogeochemical analysis of volcanic rocks allows us to describe stratified sections and reveal stages in lava eruptions resulting in a cyclic change of chemical composition of volcanic rocks (from basalts to andesites within the sequences of the Kumsa and Krasnaya Rechka structures). It should be specially noted that the rock association is constant in all considered structures.

The lava series consists of 35 lava flows with a total thickness of 1200 m in the Kumsa structure [10, 11, 14], 21 flows (560 m thick) in the Semch structure, 18 flows (630 m thick) in the Koikary structure, and 18 flows forming a 270-m volcanic section in the Krasnaya Rechka village area. Correlated sections are presented in Fig. 2.

Lava flows with thicknesses from 9–12 to 40–45 m (massive, amygdaloidal, variolitic, rarely pillow) are dominant. Tuffs form interbeds with smaller thicknesses (0.5–4.5 m) between lava breccia and are typical only of the upper parts of the sections. The proportion of pyroclastic rocks increases from the middle part of

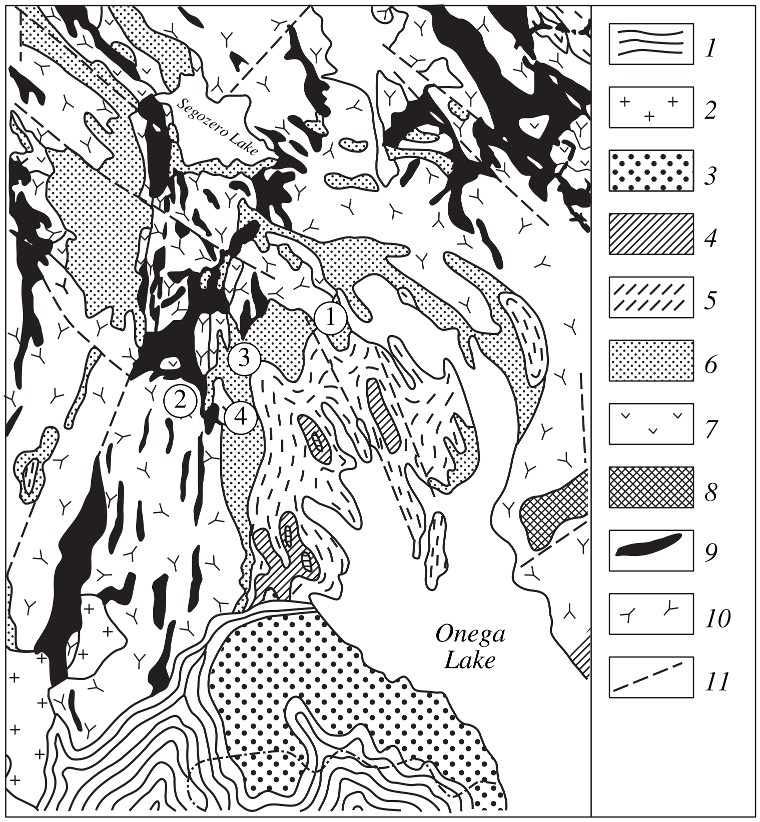

**Fig. 1.** Scheme of location of key sections of the Sumian complex [9]. (*1*) Vendian deposits; (*2*) rapakivi granite; (*3*) Vepsian deposits; (*4, 5*) Ludicovian deposits: (*4*) Suisara complex, (*5*) Zaonezhskii complex; (*6*) Yatuliiskii complex; (*7*) Sumian–Sariolian complex; (*8*) layered intrusions; (*9*) Archean greenstone belts; (*10*) nonsubdivided Archean formations; and (*11*) faults. Numbers on the scheme indicate the location of Sumian key sequences in the structures: 1, Kumsa; 2, Semch; 3, Koikary; 4, Krasnaya Rechka.

the section in the Semch structure. A lens of basaltic andesite agglomerate tuffs 42–50 m thick was revealed there; in the area of the Deya-Oya River this lens contains a relic of secondary cinder cone composed of clumpy welded tuffs of basaltic andesites with various textures (massive, amygdaloidal, and variolitic) [13, 14].

A detailed description of Sumian volcanic sequences for the individual regions of Central Karelia is given in [11–14], and we present here only brief characteristics of the most complete sequence of the Sumian volcanic association of the Kumsa structure.

The sequence comprises seven volcanic units corresponding to separate eruption stages and includes about 36 lava flows. The eruptions of each stage began with more silicic melts.

Thick (up to 50 m) lava flows of basaltic andesites are typical of the first eruption stage. The lower zones of the lava flows are composed of massive fine-grained rocks, and amygdaloidal texture with numerous chlorite–calcite and quartz–epidote amygdules (sometimes crescentic) appears only in the roof zones. That eruptions occurred under quiet conditions is evident from the significant thickness of rocks and their lateral homogeneity. The total thickness of the unit of two lava flows is 90 m.

The lava unit corresponding to the second volcanic stage is represented by a number of lava flows with differentiated inner structure. A thick (10–40 m) lava sheet (sill) lies in the base of the unit. This sheet is characterized by a microvariolitic texture resulting from the late liquid immiscibility in melt with the formation of chemically contrasting (rhyolitic) globules 0.2–0.5 cm in size. Varioles form lenslike segregations in the central parts of the flow and are scattered over the whole volume closer to the roof. Some areas of lava flows contain signs of residual laminar motion of melt. Four overlying lava flows from 10 to 30 m thick contain varioles 1–3 cm in size both as isolated globules and as segregations. Small amygdules of quartz–albite and albite composition are typical of these flows. Unique structural features of these rocks allows us to use them as markers in a lateral study of the association. Similar flows composed of microvarioles are also typical of the Koikary structure and are rare in the Semch and Krasnaya Rechka areas. The total thickness of the unit consisting of six lava flows is 250 m.

Massive homogeneous lava flows 10–100 m thick with small amygdules at the roof are typical of the third

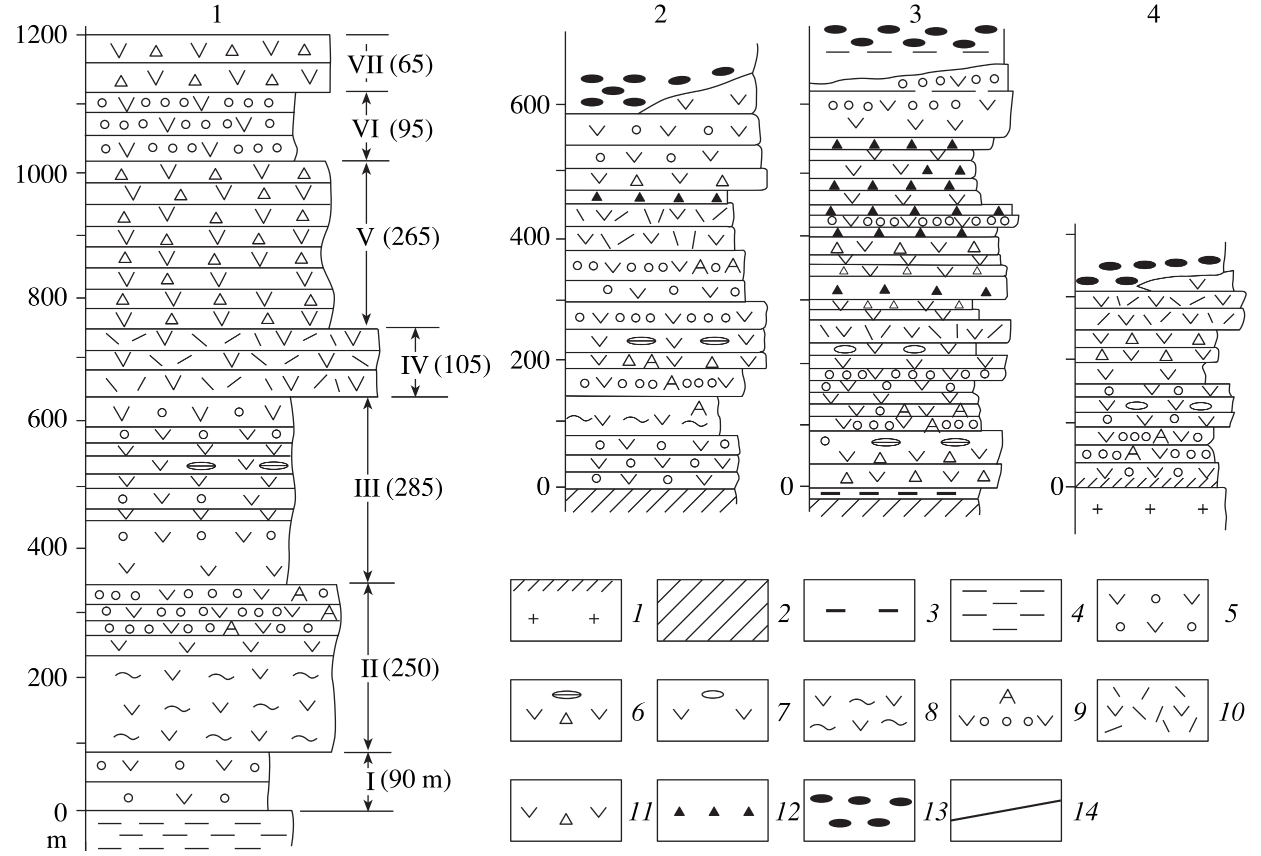

**Fig. 2.** Typical stratigraphic sections of Sumian basaltic andesites of Central Karelia. Numbers above the sections indicate: 1, Kumsa structure, after [14]; 2, Semch, after [13]; 3, Koikary, after [13]; 4, Krasnaya Rechka, after [10, 11]. Symbols: (*1*) granite, weathered rock; (*2*) Lopian deposits; (*3*) sedimentary breccia; (*4*) sediments of the Kumsa Formation, lower subformation (schist, sandstone, quartz sandstone); (*5*) massive basaltic andesite with amygdules at the roof; (*6*) massive, brecciated basaltic andesite with layered amygdules at the roof of the flow; (*7*) massive basaltic andesite with large quartz amygdules; (*8*) basaltic andesite with microvariolitic texture; (*9*) variolites with albite amygdules; (*10*) basaltic andesite with *Pl* phenocrysts; (*11*) massive brecciated lavas; (*12*) agglomerate, clumpy basaltic andesite tuff; (*13*) polymict conglomerate; and (*14*) boundaries between layers and flows.

volcanic stage. Large quartz or layered amygdules (flow 13) are rare. The total thickness of the unit (eight flows) is 285 m.

The fourth unit is composed of five lava flows with porphyritic texture formed by tabular and acicular phenocrysts of albite and albite–oligoclase up to 0.5 cm in size, which are regularly distributed over the flow thickness; small quartz amygdules occur in the roof parts of flows. This unit is a reliable marker and observed in all studied sequences. The total thickness of the unit is 105 m.

A group of lava bodies related to the fifth unit is characterized by a prevalence of brecciated textures at the roof of the flows and by the occurrence of flows entirely composed of lava breccias. The total thickness of the unit comprising eight lava flows is 265 m.

The next, sixth unit is composed of four flows of variolitic lavas from 18 to 30 m thick. Varioles 1–5 cm in size are distributed over the whole thickness of the flow, sometimes forming segregations and spots. Small quartz amygdules occur in the roof parts. The total thickness of the unit is 95 m. The second horizon of variolitic lavas also occurs in the upper part of the Semch sequence, but liquid immiscibility textures are locally seen in the middle part of the sequence.

The sequence is accomplished by two lava breccia flows with a total thickness of 65 m. The volcanic association is overlain by a series of tuffaceous conglomerates and polymict conglomerates with sandstone and gritstone beds.

Individual sections differ in some features from the most complete section in the Kumsa structure described above.

The Sumian sequence in the Semch structure begins with a brecciated lava flow, the upper part of which contains numerous layered amygdules (sometimes with geodes) helpful in revealing the primary attitude of rocks and small quartz and albite amygdules. Variolitic lavas (third flow) contain many small bright red albite amygdules in the roof part. The ninth flow is also a marker for the Semch structure. This flow contains large rounded amygdules up to 5–7 cm and, rarely, 10 cm in size. They are composed of milky white quartz and occupy up to 20–30% of the outcrop areas, so that the rocks look like conglomerates and can be easily identified in the field. Plagioclase porphyrites compose the tenth and eleventh flows and, starting from the second part of the sequence, the flows are mainly composed of lava breccias or brecciated lavas, which are separated by horizons of agglomerate and lapilli tuffs. A relic of a secondary explosive dome is mapped there. Hence the Semch structure sequence differs in a greater abundance of explosive material from the other structures, where tuff beds are normally rare and thin.

Columnar jointing is typical of the first three basaltic andesite flows in the Koikary structure sequence. A flow with layered amygdules and horizons of microvariolites and variolites also occur. Albite amygdules are abundant in the lower parts of the section with variolites and in the middle of the section. Plagioclase porphyrites form two lava flows, while massive lavas compose the upper part of the section.

Variolitic lavas with pink albite amygdules compose the second and third flows of the Krasnaya Rechka sequence. Large quartz amygdules are typical of the fifth and sixth flows. They are followed by the flows with lava breccias in the roof parts, while plagioclase porphyrites form the eleventh and twelfth flows.

It is important to emphasize that the markers (variolitic lavas and plagioclase porphyrite flows) distinguished in individual sections can only help in the correlation of whole units within the distant structures. For example, plagioclase porphyrites appear at a level of 625 m from the section base in the Kumsa structure, at 220 m in the Semch structure, and at 470 m in the Koikary structure. These rocks are traced laterally for 1.5–10 km, which allows one to use them as marker horizons during the study of local objects.

The rocks of the studied association underwent metamorphism of greenschist to epidote amphibolite facies. The mineral assemblage of groundmass mainly comprises hornblende (actinolite), chlorite, epidote, biotite, plagioclase (albite and albite–oligoclase), and accessory mineral phases (magnetite, titanite, pyrite, and chalcopyrite).

Unfortunately, there are no isotopic data on the age of the Sumian basaltic andesite association of Central Karelia. However, the following data were obtained by the Sm–Nd method for rocks of the same stratigraphic level in Eastern Karelia (Vetrenyi Belt Formation): 2448 ± 42 Ma for the lower part of the section and 2410 ± 34 Ma for its upper part [15–17]. Comagmatic intrusions of the Karelian craton have similar ages of 2.45–2.435 Ma [18]. Sumian basalts are abundant at the base of the Imandra–Varzuga complex in the Kola geoblock. They also occur in the Keulik and Kinirim sequences and are replaced by basaltic andesites in the upper parts of the sequences. Their age is 2442 ± 1.7 Ma [18].

## STUDY METHODS

30 samples were collected for geochemical study from poorly metamorphosed volcanic rocks of different facies and textural features in the Krasnaya Rechka structure. Samples with evident metasomatic alteration were excluded after petrographic study.

Geochemical study comprised the analysis of major and trace elements by the X-ray fluorescent method (VRA-33) in the Institute of Geology, Russian Academy of Sciences, Karelian Research Center, Petrozavodsk. The error was <2% for elements with concentrations of >0.5 wt %, 3% at concentrations of >30 ppm, and 5% at concentrations of <30 ppm. Trace elements and REEs were determined by ICP-MS at the Institute of Geology of Ore Deposits, Petrography, Mineralogy, and Geochemistry, Russian Academy of Sciences, Moscow. The error of element analysis was <3%.

Mg# was calculated by the formula $100Mg^{2+}/(Mg^{2+} + Fe^{2+})$, at. %; $Hf/Hf^* = Hf_n/[Nd_nSm_n]^{1/2}$, $Ta/Ta^* = Ta_n/[Th_nLa_n]^{1/2}$, $Ti/Ti^* = Ti_n/[Eu_n^* Tb_n]^{1/2}$. The element concentrations were normalized to the composition of primitive mantle [19].

The previously published data on the Koikary, Semch, and Kumsa structures obtained by X-ray fluorescence (VRA-33) in the Institute of Geology, Russian Academy of Sciences, Karelian Research Center, were additionally used for a geochemical description of the Sumian associations [11, 14].

## GEOCHEMICAL CHARACTERISTICS OF THE ASSOCIATION

The Sumian volcanic rocks described above have a number of unique geochemical features, such as high MgO and Cr concentrations combined with high $SiO_2$ and low HREE contents.

The volcanic rocks of the association contain 48–58 wt % $SiO_2$ and belong to the basalt–basaltic andesite–andesite series with normal alkalinity ($Na_2O + K_2O$ = 2–5 wt %). The average $SiO_2$ content is as follows: 53.56 ± 2.34 wt % for Krasnaya Rechka (table), 55.20 ± 3.18 wt % for Kumsa, 56.26 ± 2.15 wt % for Koikary, and 55.08 ± 1.06 wt % for Semch. The average $TiO_2$ content is 0.86 ± 0.19 wt % for Krasnaya Rechka, 0.82 ± 0.24 wt % for Kumsa, 0.83 ± 0.21 wt % for Koikary, and 1.01 ± 0.10 wt % for Semch. The average MgO content is 5.59 ± 0.99 wt % for Krasnaya Rechka, 5.67 ± 1.87 wt % for Kumsa, 6.21 ± 2.42 wt % for Koikary, and 5.90 ± 0.98 wt % for Semch, at the highest values of 9.55–10.33 wt %. However, basalts are present only in sequences of the Krasnaya Rechka and Kumsa structures, whereas in the other cases the association comprises only basaltic andesites and andesites.

Representative compositions of rocks of basaltic andesite association of the Krasnaya Rechka structure (wt %, ppm)

| Component | Sample | | | | | | | | | |
|---|---|---|---|---|---|---|---|---|---|---|
| | 508-3 | 508-4 | 508-6 | 508-11 | 506-18 | 506-23 | 506-25 | 506-27 | 506-29 | 506-30 |
| | Level | | | | | | | | | |
| | 1 | | | | 2 | | | | | |
| $SiO_2$ | 49.98 | 50.72 | 53.26 | 56.70 | 49.52 | 56.06 | 54.16 | 53.60 | 56.04 | 55.30 |
| $TiO_2$ | 1.26 | 1.24 | 1.02 | 1.09 | 0.88 | 0.94 | 0.90 | 0.83 | 0.92 | 0.93 |
| $Al_2O_3$ | 15.94 | 16.20 | 14.29 | 13.97 | 12.27 | 12.76 | 12.83 | 12.31 | 12.83 | 14.14 |
| $Fe_2O_3$ | 7.82 | 3.05 | 6.30 | 4.14 | 2.81 | 1.94 | 5.17 | 1.19 | 1.06 | 1.38 |
| FeO | 6.10 | 7.06 | 7.29 | 4.91 | 10.34 | 8.69 | 4.89 | 8.74 | 8.05 | 8.12 |
| MnO | 0.16 | 0.17 | 0.13 | 0.11 | 0.21 | 0.18 | 0.19 | 0.20 | 0.17 | 0.16 |
| MgO | 5.50 | 6.70 | 6.63 | 5.34 | 9.08 | 5.70 | 7.06 | 8.47 | 6.60 | 5.29 |
| CaO | 2.80 | 3.08 | 1.54 | 3.08 | 7.43 | 5.54 | 7.15 | 7.29 | 6.10 | 6.24 |
| $Na_2O$ | 5.46 | 4.26 | 3.18 | 3.81 | 1.00 | 4.11 | 3.46 | 3.88 | 4.82 | 3.57 |
| $K_2O$ | 0.50 | 0.94 | 1.41 | 1.25 | 3.29 | 1.31 | 2.08 | 0.60 | 1.02 | 2.60 |
| $H_2O$ | 0.26 | 0.18 | 0.26 | 0.16 | 0.03 | 0.13 | 0.10 | 0.10 | 0.13 | 0.08 |
| LOI | 4.41 | 6.00 | 4.48 | 5.02 | 2.70 | 2.16 | 1.56 | 2.38 | 1.87 | 1.85 |
| Total | 100.19 | 99.60 | 99.79 | 99.58 | 99.56 | 99.52 | 99.55 | 99.59 | 99.61 | 99.66 |
| Mg# | 42.73 | 54.91 | 47.69 | 52.52 | 55.70 | 49.32 | 56.87 | 60.61 | 56.64 | 50.17 |
| Cr | 25 | 15 | 42 | 34 | 406 | 225 | 303 | 391 | 82 | 67 |
| Co | 63.7 | 74.1 | 59.3 | 48.8 | 71.5 | 54.8 | 52.6 | 59.2 | 53.2 | 48 |
| Pb | – | – | – | – | 59 | 50 | – | – | 40 | – |
| Rb | – | – | 46 | – | – | – | – | – | – | – |
| Ba | 402 | 554 | 465 | 629 | 1928 | 696 | 1108 | 456 | 744 | 3569 |
| Ti | 7547 | 7428 | 6110 | 6529 | 5271 | 5631 | 5391 | 4972 | 5511 | 5571 |
| Th | 4.6 | 4.4 | 4.4 | 3.5 | 2.4 | 3.7 | 3.6 | 2.7 | 3.1 | 3.9 |
| U | 1.6 | – | 0.9 | – | – | 1.6 | – | 0.8 | 0.6 | – |
| Ta | 1.1 | 0.93 | 0.72 | 0.75 | 0.49 | 0.58 | 0.49 | 0.45 | 0.61 | 0.53 |
| Cs | – | – | – | – | 3.3 | – | 1.3 | – | 1.1 | – |
| Hf | 4.7 | 4.1 | 4.1 | 3.0 | 3.2 | 3.1 | 2.6 | 2.3 | 3.6 | 3.4 |
| Sc | 21.5 | 24.3 | 17.7 | 24.5 | 23.3 | 23.2 | 24.3 | 30.4 | 26.6 | 21.5 |
| La | 12.2 | 74.1 | 39.8 | 57.3 | 39.0 | 21.4 | 24.6 | 8.8 | 9.4 | 14.3 |
| Ce | 31.3 | 113.7 | 66.2 | 98.8 | 67.1 | 34.4 | 36.5 | 20.4 | 18.8 | 32.7 |
| Nd | 27 | 58 | 42 | 59 | 42 | 22 | 26 | 11 | 12 | 20 |
| Sm | 4.87 | 9.07 | 6.29 | 10.69 | 7.05 | 4.11 | 4.51 | 3.28 | 3.02 | 3.89 |
| Eu | 1.71 | 2.23 | 1.9 | 3.31 | 1.91 | 1.37 | 1.29 | 0.9 | 0.76 | 0.88 |
| Tb | 0.63 | 0.52 | 0.58 | 0.82 | 0.52 | 0.34 | 0.39 | 0.54 | 0.25 | 0.31 |
| Yb | 2.1 | 1.7 | 2.3 | 1.7 | 1.4 | 1.6 | 1.6 | 1.2 | 1.3 | 1.3 |
| Lu | 0.37 | 0.27 | 0.29 | 0.25 | 0.27 | 0.29 | 0.29 | 0.26 | 0.29 | 0.25 |

**Table.** (Contd.)

| Component | Sample | | | | | | | | | |
|---|---|---|---|---|---|---|---|---|---|---|
| | 506-31 | 506-33 | 506-34 | 506-35 | 506-37 | 506-42 | 506-44 | 506-73 | 506-75 | 506-76 |
| | Level | | | | | | | | | |
| | 3 | | | | | | | | | |
| $SiO_2$ | 55.22 | 51.58 | 54.50 | 51.58 | 49.40 | 54.78 | 56.92 | 58.16 | 50.26 | 46.06 |
| $TiO_2$ | 1.00 | 1.12 | 1.03 | 1.06 | 1.14 | 1.07 | 0.84 | 0.89 | 1.05 | 1.10 |
| $Al_2O_3$ | 15.45 | 14.14 | 13.62 | 15.45 | 16.74 | 14.25 | 13.87 | 13.57 | 15.03 | 16.05 |
| $Fe_2O_3$ | 1.94 | 1.96 | 1.26 | 1.42 | 1.39 | 1.82 | 2.97 | 1.71 | 1.73 | 1.93 |
| FeO | 7.26 | 10.66 | 9.94 | 9.70 | 11.25 | 9.33 | 7.41 | 6.47 | 10.77 | 12.21 |
| MnO | 0.15 | 0.20 | 0.17 | 0.22 | 0.23 | 0.19 | 0.17 | 0.17 | 0.23 | 0.26 |
| MgO | 4.18 | 5.70 | 5.44 | 5.56 | 5.29 | 4.83 | 4.60 | 4.10 | 6.07 | 6.95 |
| CaO | 6.10 | 6.24 | 5.33 | 5.26 | 4.70 | 4.56 | 5.18 | 6.16 | 4.76 | 4.76 |
| $Na_2O$ | 5.40 | 3.43 | 4.88 | 4.36 | 4.33 | 4.18 | 3.50 | 4.21 | 4.03 | 4.08 |
| $K_2O$ | 0.60 | 1.40 | 1.00 | 2.10 | 1.72 | 1.72 | 1.90 | 1.10 | 1.26 | 1.02 |
| $H_2O$ | 0.13 | 0.13 | 0.12 | 0.15 | 0.16 | 0.21 | 0.18 | 0.16 | 0.26 | 0.30 |
| LOI | 2.44 | 2.97 | 2.35 | 3.15 | 3.63 | 2.65 | 2.35 | 3.43 | 4.36 | 5.41 |
| Total | 99.87 | 99.53 | 99.64 | 100.01 | 99.98 | 99.59 | 99.89 | 100.13 | 99.81 | 100.13 |
| Mg# | 45.27 | 44.98 | 46.68 | 47.44 | 42.99 | 43.97 | 44.84 | 47.71 | 46.74 | 47.03 |
| Cr | 65 | 51 | 64 | 52 | 54 | 58 | 61 | 85 | 60 | 59 |
| Co | 41.5 | 57.3 | 55.7 | 53 | 65.3 | 53.2 | 47.8 | 44.4 | 65.6 | 68.9 |
| Pb | – | – | – | – | – | – | – | – | – | – |
| Rb | – | 38 | 23 | 51 | 37 | 31 | 83 | 52 | 35 | – |
| Ba | 381 | 853 | 550 | 655 | 364 | 372 | 411 | 405 | 447 | 438 |
| Ti | 5990 | 6709 | 6170 | 6349 | 6829 | 6409 | 5032 | 5331 | 6290 | 6589 |
| Th | 3.9 | 4.1 | 4.5 | 3.8 | 4.2 | 4.0 | 3.5 | 3.6 | 4.4 | 3.4 |
| U | – | 0.7 | – | – | – | 0.5 | 2.2 | 0.8 | 0.6 | 0.5 |
| Ta | 0.67 | 0.67 | 0.99 | 0.65 | 0.64 | 0.58 | 0.53 | 0.74 | 0.71 | 0.7 |
| Cs | – | – | – | – | 1.9 | 1.4 | 1.6 | 1.4 | – | – |
| Hf | 3.3 | 3.8 | 3.8 | 3.6 | 4.0 | 3.8 | 3.1 | 3.7 | 4.1 | 3.8 |
| Sc | 19.3 | 21.2 | 20.2 | 19.9 | 20.7 | 19.6 | 18.4 | 21.5 | 22.0 | 21.5 |
| La | 22.2 | 20.2 | 12.4 | 39.6 | 20.4 | 18.1 | 35.3 | 27.1 | 17.7 | 19.4 |
| Ce | 37.7 | 43 | 23.2 | 73.9 | 35.4 | 34.1 | 61.7 | 47.1 | 28.3 | 31.4 |
| Nd | 26 | 32 | 28 | 47 | 25 | 23 | 39 | 33 | 21 | 22 |
| Sm | 5.03 | 6.01 | 4.22 | 7.03 | 4.95 | 4.39 | 7.31 | 6.3 | 4.42 | 4.84 |
| Eu | 2.05 | 1.8 | 0.97 | 2.37 | 1.7 | 1.15 | 2.6 | 1.86 | 0.91 | 0.98 |
| Tb | 0.51 | 0.96 | 0.35 | 0.66 | 0.59 | 0.46 | 0.64 | 0.68 | 0.29 | 0.58 |
| Yb | 1.6 | 1.6 | 1.6 | 1.6 | 1.9 | 1.4 | 1.7 | 1.9 | 1.8 | 2.1 |
| Lu | 0.28 | 0.29 | 0.26 | 0.25 | 0.31 | 0.24 | 0.28 | 0.3 | 0.32 | 0.23 |

Note: Level is the position of the sample in stratigraphic section: (1) the base, (2) the middle part, and (3) the upper part. Samples 508-3, 508-4 are fine-grained basalt from the base of the flow; sample 508-6 is fine-grained basaltic andesite with variolitic texture; samples 508-11 and 506-23 are fine-grained basaltic andesites from the base of the flow; sample 506-18 is fine-grained basalt from the central part of the flow; samples 506-25, 506-27, 506-29, and 506-30 are fine-grained basaltic andesites from the base of the flow; samples 506-31, 506-34, and 506-42 are basaltic andesites with *Pl* phenocrysts from the base of the flow; samples 506-33, 506-35, and 506-76 are basalts with *Pl* phenocrysts from the base of the flow; samples 506-37 and 506-75 are basalts with *Pl* phenocrysts from the central part of the flow; sample 506-44 is andesite with *Pl* phenocrysts from the central part of the flow; and sample 506-73 is andesite with *Pl* phenocrysts from the roof of the flow.

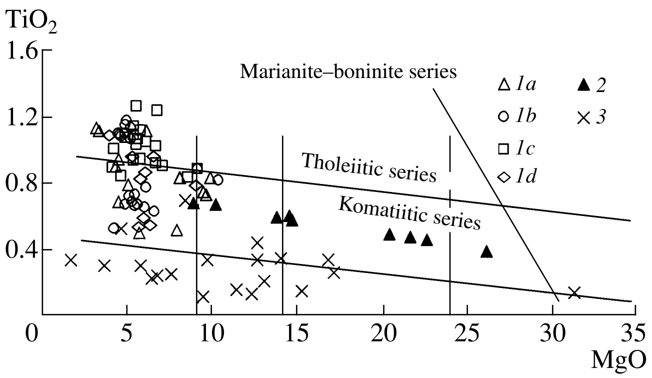

**Fig. 3.** $TiO_2$–MgO diagram. Sumian basaltic andesites of Central Karelia from different structures: (*1a*) Koikary, (*1b*) Semch, (*1c*) Krasnaya Rechka, (*1d*) Kumsa, (*2*) komatiite of the Vetrenyi Belt [17], and (*3*) boninite of the Mariana Trough [21].

The volcanic phases in the Semch structure are distinguished by $TiO_2$ and MgO concentrations: $TiO_2$ 1.13–1.18 wt %, MgO 5.14–4.94 wt % (the first phase); $TiO_2$ 0.81–1.10 wt %, MgO 10.33–4.44 wt % (the second phase); $TiO_2$ 0.86–1.09 wt %, MgO 9.07–4.49 wt % (the third phase); $TiO_2$ 0.62–0.73 wt %, MgO 6.56–4.81 wt % (the fourth phase).

The $CaO/Al_2O_3$ ratio in volcanic rocks is <0.5 for Krasnaya Rechka, <0.6 for Kumsa, and <0.7 for Semch and Koikary. The $Al_2O_3/TiO_2$ ratio is 12–15 for Krasnaya Rechka and 12–24 for Semch and Koikary.

Points of Sumian volcanic rocks form an area at the boundary between the komatiitic and tholeiitic series in the $TiO_2$–MgO diagram (Fig. 3) [20]. The trends for the described volcanic series strongly differ from those for boninite magmas from the Western Pacific island arc (Bonin Island, Mariana Trough) [21] and komatiites of the Vetrenyi Belt with a similar age of 2410 ± 34 Ma [17].

The volcanic rocks of the boninitic series from the Bonin arc (Japan) have >9 wt % MgO at >55 wt % $SiO_2$ and a low $TiO_2$ content (<0.3 wt %) [22]. Volcanic rocks with similar lithogeochemical features were found on Cape Vogel, Papua New Guinea [23], dredged from the bottom of the Mariana Trough, and obtained by deep-sea drilling (DSDP site 458) in the Marian forearc zone [21]. The data obtained demonstrated significant variations in the composition of the volcanic rocks and the following geochemical requirements were formulated for distinguishing the "boninite-like" series: MgO 9–25 wt %, $SiO_2 > 52$ wt %, $TiO_2 < 0.4$ wt %, Ni 70–450 ppm, and Cr 200–1800 ppm. The international classification recommends using the following parameters: MgO > 8%, $SiO_2 > 52\%$, and $TiO_2 < 0.5\%$ [21, 24].

The rocks of the Sumian basaltic andesite associations of Central Karelia show some differences compared to boninites from Tonga arc [25, 26] and Archean boninites from Abitibi [2]. The average MgO content in the studied volcanic rocks is significantly lower than 9 wt %, Mg# < 50 (>60 in boninites after [3] and >75 in the Archean boninites from Abitibi [2]). $TiO_2$ contents of 0.6–1.3 wt % are higher and more variable than in boninites. Concentrations of Ni (135 ± 70 ppm for Koikary and 114 ± 52 ppm for Semch) and Cr (112 ± 92 ppm for Krasnaya Rechka and 295 ± 134 ppm for Koikary) also do not meet the classification requirements for the rocks of the boninitic series.

The $K_2O/Na_2O$ ratio for Sumian volcanic rocks is <0.75 (0.35 ± 0.14 for Krasnaya Rechka, 0.4 ± 0.29 for Kumsa, 0.22 ± 0.19 for Koikary, and 0.41 ± 0.13 for Semch), which is close to those in volcanic rocks from active continental margins ($K_2O/Na_2O$ = 0.2–0.4) and volcanic arcs on margins of plates ($K_2O/Na_2O$ = 0.5) [27, 28].

Ti/Zr ratios in Sumian basaltic andesites are 52.91 ± 4.21, Zr/Y = 6.34 ± 0.92, and Hf/Th = 0.93 ± 0.12, which significantly differ from those in boninites (Ti/Zr = 70–110, Zr/Y = 0.9–1.9, and Hf/Th > 3) and are similar to these ratios in volcanic rocks of active continental margins (Ti/Zr = 49–65, Zr/Y = 5–8, Hf/Th = 0.99 ± 0.26) [28].

The rocks of the basaltic andesite associations from Central Karelia on the Zr–3Y–Ti/100 and Zr–Sr/2–Ti/100 graphs (Fig. 4) plot together with boninites of the Mariana Trough to the CAB area, on the boundary with WPB.

The REE distribution over the section (its lower, middle, and upper parts) is topologically similar (Fig. 5). However, the REE contents vary: $(La/Sm)_n$ = 1.6–5.2 and $(Ce/Yb)_n$ = 5.1–16.1 for the lower part of the section, $(La/Sm)_n$ = 1.7–3.5 and $(Ce/Yb)_n$ = 4.1–6.8 for the middle part of the section, and $(La/Sm)_n$ = 1.8–3.1 and $(Ce/Yb)_n$ = 5.2–6.8 for the upper part of the section. The distribution of HREE contents is more homogeneous: $(HREE)_n$ = 0.81 ± 0.08 for the lower part of the section, $(HREE)_n$ = 0.60 ± 0.07 for the middle part of the section, and $(HREE)_n$ = 0.72 ± 0.07 for the upper part of the section. According to the type of REE spectra, Sumian basaltic andesites from Central Karelia strongly differ from boninites and LREE-enriched Proterozoic komatiites of similar age from the Vetrenyi Belt (Fig. 6).

The rocks from different parts of the section show similar trace-element spectra (Fig. 6). Negative Ta, Hf, and Ti anomalies are distinct: Hf/Hf* = 0.63 ± 0.32, Ta/Ta* = 0.43 ± 0.23, and Ti/Ti* = 0.62 ± 0.15 at the base of the section; Hf/Hf* = 0.61 ± 0.32, Ta/Ta* = 0.42 ± 0.24, and Ti/Ti* = 0.62 ± 0.15 in the middle part of the section; Hf/Hf* = 0.76 ± 0.21, Ta/Ta* = 0.44 ± 0.14, and Ti/Ti* = 0.73 ± 0.29 in the upper part of the section. The character of trends differs from that of volcanic rocks of the Vetrenyi Belt.

The search for possible analogues demonstrated the closest similarity of Sumian basaltic andesite association to basalts and andesites of active continental margins of the Western Pacific (Andean) type by geochem-

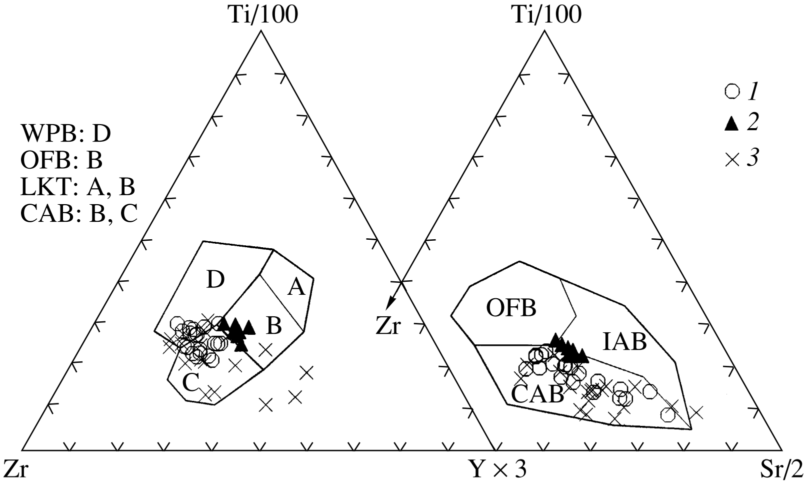

**Fig. 4.** Zr–Y3–Ti/100 and Zr–Ti/100–Sr/2 diagrams for distinguishing the geodynamic setting of volcanic series. (*1*) Basaltic andesite of Krasnaya Rechka, (*2*) komatiite of the Vetrenyi belt [17], and (*3*) boninite of the Mariana Trough [21]. WPB are within-plate basalts, OFB are ocean-floor basalts, LKT are low-K tholeiites, CAB are calc-alkaline basalts, and IAB are island-arc basalts.

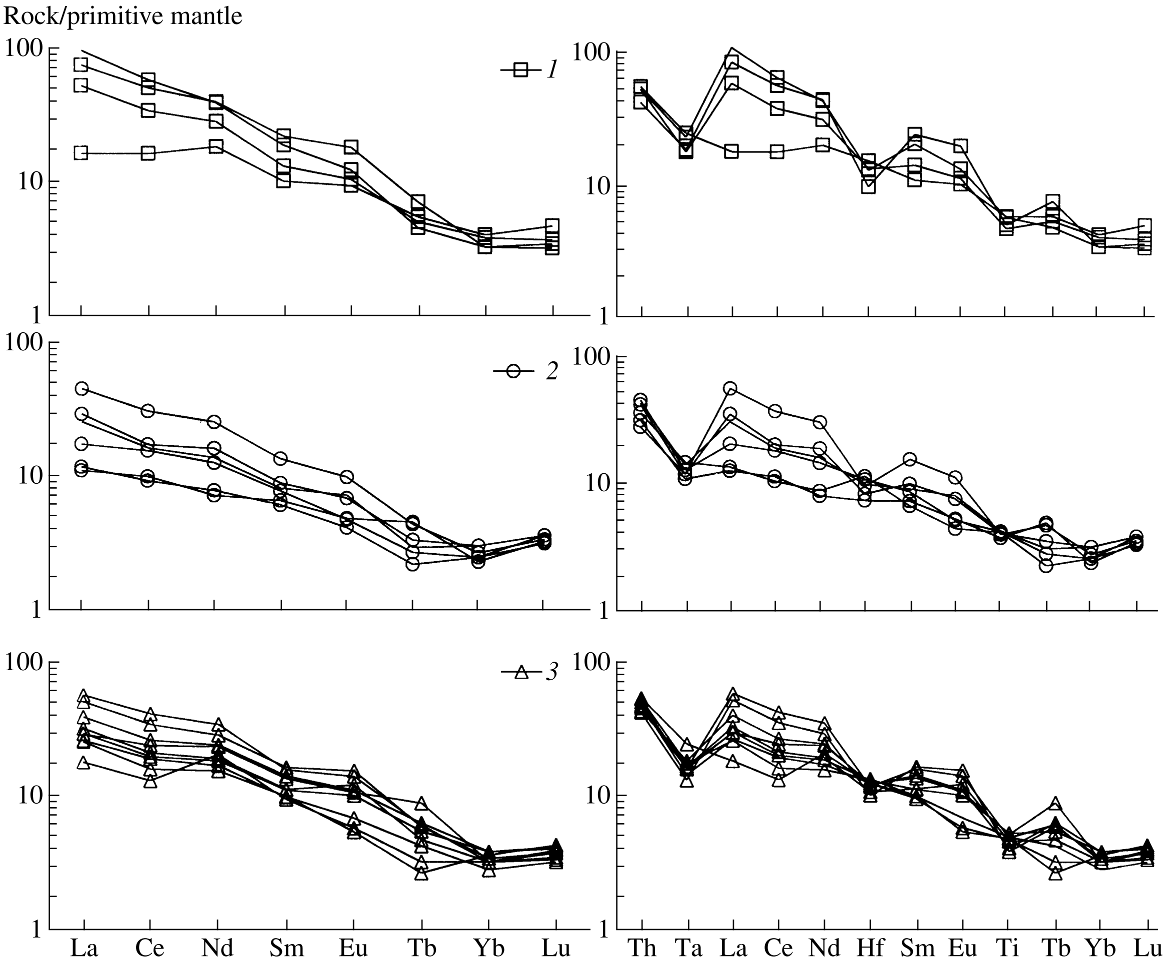

**Fig. 5.** Distribution of REE and minor elements over the basaltic andesite sequence in the Krasnaya Rechka structure. (*1*) Lower part of the sequence, (*2*) middle part of the sequence, and (*3*) upper part of the sequence. Normalized to primitive mantle [19].

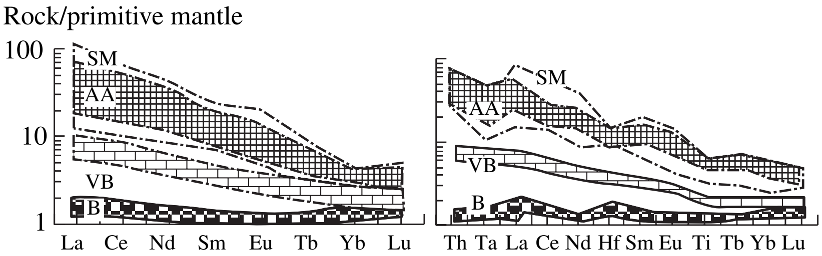

**Fig. 6.** Distribution of REE and minor elements in Sumian volcanics from Central and Eastern Karelia as compared with boninites from the Mariana Trough [20] and basaltic andesites from the Andean active continental margin [27]. Normalized to primitive mantle [18]. SM are Sumian basaltic andesite from Central Karelia, VB are komatiites from the Vetrenyi Belt, B are boninites from the Mariana Trough, and AA are basaltic andesites from the Andean active continental margin.

ical features, REE, and trace elements. The similarity is expressed in high contents of LILE (Rb 23–90, Ba 380–3500, Sr 310–628, and Th 2.4–4.6) comparable with those in volcanic rocks from active continental margins, as well as in HFSE contents (Ta 0.4–0.9, Ce 20–113, Zr 91–129, Hf 2.3–4.1, Y 15–29, Yb 1.2–2.1, and Sc 17.7–30.4) higher than in analogous island arc series and similar to those in rocks of active continental margins.

## THE CONDITIONS OF MAGMA GENESIS

Discussion of specific geochemical features of Sumian basaltic andesite association requires characterization of the magma genesis conditions, which can be modeled using the Pele version 4.0 software (Duke University).

Model temperatures of initial magma eruption varied in the range of 1150– 1200°C depending directly on the melt basicity. Magma during its eruption had a density of 2.54–2.69 g/cm$^3$ and viscosity of ~5.3–8.3 P with this value being twice as high as the viscosity calculated for the melt of komatiitic basalt from the Vetrenyi Belt (2.6 P) with a similar magnesia content (≅99 wt %) and density (2.68 g/cm$^3$).

The higher viscosity of erupting magma resulted in the formation of poorly differentiated thick lava flows. The erupting magmas were rich in volatiles, and the melt motion was laminar, which is evident from the distribution of amygdules in lavas.

The calculated temperature of magma generation was 1250–1380°C. However, these values may be overestimated, because the $H_2O$ content in the initial melt was not considered in the calculation, but could be significant, as is testified by the presence of relics of initial amphibole (hornblende) in several lava flows.

Modern experimental data demonstrate that $H_2O$ solubility may reach 3–6 wt % for andesite melts at a pressure of ~3–5 kbar and temperature of 1100–1150°C [29]. Such contents may decrease the melting temperature by 100–150°C, and we can suppose a shallow-level magma genesis.

Thus, geological, facial, petrographic, and geochemical data may indicate the formation of Sumian volcanic rocks in the geodynamic conditions comparable to those in an Andean-type active continental margin. The depth of magma generation in such zones is estimated as 80–100 km, which is consistent with the presence of basalts as products of deep magmatic melts. At the same time, low-velocity zones are established in the continental crust of the Central Andes at depths of 10–35 km. These zones are interpreted as intermediate magma chambers, the areas of potential accumulation of melts [30]. Contamination of basaltic magma by crustal material and its further differentiation occur at this depth, which causes a predominance of basaltic andesite and andesite melts during the eruptions. Initial basaltic melts (untouched by crustal contamination) could rarely reach the surface and preserved their high MgO, Ni, and Cr concentrations during the eruptions.

## CONCLUSIONS

(1) A large Paleoproterozoic province of basaltic andesites was formed at 2.55–2.40 Ga within the Karelian craton.

(2) Geochemical features of basaltic andesite associations of Central Karelia differ strongly from those of the boninite series by MgO content <9 wt %, $SiO_2$ 46–58 wt %, Mg# < 60, $TiO_2$ = 0.8–1.3 wt %, Hf < 4.2 ppm, Ta < 0.7 ppm, Zr < 120 ppm, and by the topology of REE and trace-element spectra. The closest geochemical similarity of Sumian volcanic rocks is established with basaltic andesites of the Andean-type active continental margins.

(3) The temperature of erupted melts reached 1150–1200°C, their densities ranged within 2.54–2.69 g/cm$^3$ at viscosities of 5.3–8.3 P, which resulted in the formation of poorly differentiated thick lava flows. The volcanic rocks of the Sumian association of Central Karelia were formed during several stages with relatively short hiatuses. The magmas were erupted in a subaerial environment from separate distant volcanic centers.

The igneous rock series were formed by similar processes of magma differentiation.

(4) The proposed models suggest shallow depths of magma generation, the presence of water in magmas, and a significant degree of crustal contamination, which are also typical of the subduction-related volcanic rocks.

These conclusions will help in the reconstruction of geodynamic regimes in Eastern Fennoscandia within the range of 2.5–2.4 Ga and will be combined with detailed isotopic dating of the volcanic sequences and a petrological and geochemical correlation of the studied associations with volcanic complexes of the same age in this region. These studies will be continued within the frames of the RFBR project no. 02-05-65052.

## ACKNOWLEDGMENTS

The study was supported by the Russian Foundation for Basic Research (project nos. 98-05-03543, 01-05-64228, 02-05-65052, 02-05-97507). S.A. Svetov thanks the Russian Science Support Foundation for financial assistance.

## REFERENCES

1. A. Riganti and A. H. Wilson, "Geochemistry of the Mafic–Ultramafic Volcanic Associations of the Nondweni Greenstone Belt, South Africa, and Constraints on Their Petrogenesis," Lithos **34**, 235–252 (1995).
2. R. Kerrich, D. Wyman, J. Fan, and W. Bleeker, "Boninite Series: Low Ti-Tholeiite Associations from the 2.7 Ga Abitibi Greenstone Belt," Earth Planet. Sci. Lett. **164**, 303–316 (1998).
3. A. A. Shchipanskii, A. V. Samsonov, M. M. Bogina, *et al.*, "High-Mg, Low-Ti Quartz Amphibolites of the Khizovaara Greenstone Belt, Northern Karelia: Archean Metamorphosed Boninites?," Dokl. Akad. Nauk **365** (6), 817–820 (1999) [Dokl. Earth Sci. **365A** (3), 422–425 (1999].
4. A. A. Shchipanskii, I. I. Babarina, K. A. Krylov, *et al.*, "The Oldest Ophiolites: The Late Archean Suprasubduction Zone Complex of the Iringora Structure, North Karelian Greenstone Belt," Dokl. Earth Sci. **377A** (3), 283–287 (2001).
5. A. J. Crawford, T. J. Fallon, and D. H. Green, "Classification, Petrogenesis and Tectonic Setting of Boninites," in *Boninites* (Unwin Hyman, London, 1989), pp. 2–44.
6. J.-L. Poideven, "Boninite-like Rocks from the Palaeoproterozoic Greenstone Belt of Bogoin, Central African Republic, Geochemistry and Petrogenesis," Precambrian Res. **68**, 97–113 (1994).
7. E. V. Sharkov, V. F. Smol'kin, and I. S. Krasivskaya, "Early Proterozoic Magmatic Province of High-Mg Boninite-like Rocks in the Eastern Baltic Shield," Petrologiya **5**, 503–522 (1997) [Petrology **5**, 448–465 (1997)].
8. D. C. Vogel, J. I. Vuollo, T. T. Alapieti, and R. S. James, "Tectonic, Stratigraphic, and Geochemical Comparisons between ca. 2500–2440 Ma Mafic Igneous Events in the Canadian and Fennoscandian Shields," Precambrian Res. **92**, 89–116 (1998).
9. *The Geology of Karelia* (Nauka, Leningrad, 1977), Ed. by V. A. Sokolov [in Russian].
10. *Problems in the Geology of Middle Proterozoic of Karelia,* Ed. by V. A. Sokolov (Kareliya, Petrozavodsk, 1972) [in Russian].
11. A. I. Golubev and A. P. Svetov, "Morphology and Chemistry of Sumian–Sariolian Sedimentary–Volcanic Sequences in the Northwestern Onega Region," in *The Geology and Mineral Deposits of Karelia* (Kareliya, Petrozavodsk, 1975), pp. 32–37.
12. K. I. Kheiskanen, A. I. Golubev, and L. F. Bondar', *Orogenic Volcanism of Karelia* (Nauka, Leningrad, 1977) [in Russian].
13. A. I. Svetova, "Andesites and Basalts in the Area of Semch River, Central Karelia," in *Geological and Petrographic Data Obtained in 1980* (Karel. Nauch. Tsentr, Petrozavodsk, 1982), pp. 23–29.
14. V. I. Korosov, *The Geology of Pre-Yatulian Proterozoic Complex in the Eastern Part of Baltic Shield (Sumian and Sariolian)* (Karel. Nauch. Tsentr, Petrozavodsk, 1991) [in Russian].
15. I. S. Pukhtel', D. Z. Zhuravlev, V. S. Kulikov, and V. V. Kulikova, "The Petrography and Sm–Nd Age of a Differentiated Komatiitic Flow of the Vetrenyi Belt, Baltic Shield," Geokhimiya, No. 5, 625–634 (1991).
16. S. A. Svetov, A. I. Golubev, and A. I. Svetova, "Geochemistry of Sumian Basalts in Central Karelia," in *Geology and Mineral Deposits of Karelia* (Karel. Nauch. Tsentr Ross. Akad. Nauk, Petrozavodsk, 2001), Vol. 4, pp. 18–26.
17. I. S. Puchtel, A. W. Hofmann, K. Mezger, *et al.*, "Petrology of a 2.41 Ga Remarkably Fresh Komatiitic Basalt Lava Lake in Lion Hills, Central Vetrenyi Belt, Baltic Shield," Contrib. Mineral Petrol. **124**, 273–290 (1996).
18. Y. V. Amelin, L. M. Neaman, and V. S. Semenov, "U–Pb Geochronology of Layered Intrusions in the Eastern Baltic Shield: Implications for the Timing and Duration of Paleoproterozoic Continental Rifting," Precambrian Res. **75**, 31–46 (1995).
19. S.-S. Sun and W. F. McDonough, "Chemical and Isotopic Systematics of Oceanic Basalts: Implications for Mantle Composition and Processes," in *Magmatism in the Ocean Basins*, Geol. Soc. Spec. Publ., No. 42, 313–345 (1989).
20. *Komatiites,* Ed. by N. T. Arudt and E. G. Nisbet (Allen and Unwin, London, 1982).
21. R. L. Hickey and F. A. Frey, "Geochemical Characteristics of Boninite Series Volcanics: Implication for Their Source," Geochim. Cosmochim. Acta. **46**, 2099–2115 (1982).
22. K. Shiraki and N. Kuroda, "The Boninite Revisited," J. Geol. Soc. Japan **86**, 34–55 (1977).

23. G. A. Jenner, "Geochemistry of High-Mg Andesites from Cape Vogel, Papua New Guinea," Chem. Geol. **33**, 307–332 (1981).

24. M. J. Le Bas, "IUGS Reclassification of the High-Mg and Picritic Volcanic Rocks," J. Petrol. **41**, 1467–1470 (2000).

25. T. J. Fallon and A. J. Crawford, "The Petrogenesis of High-Calcium Boninite Lavas Dredged from the Northern Tonga Ridge," Earth Planet. Sci. Lett. **102**, 375–394 (1991).

26. A. V. Sobolev and L. V. Danyushevsky, "Petrology and Geochemistry of Boninites from the North Termination of the Tonga Trench: Constraints on the Generation Conditions of Primary High-Ca Boninite Magmas," J. Petrol. **35**, 1183–1211 (1994).

27. O. A. Bogatikov and A. A. Tsvetkov, *Magmatic Evolution of Island Arcs* (Nauka, Moscow, 1988).

28. T. I. Frolova and I. A. Burikova, *Magmatic Associations of Modern Tectonic Environments* (Mosk. Gos. Univ., Moscow, 1997).

29. G. Moore and I. S. E. Carmichael, "The Hydrous Phase Equilibria (to 3 kbar) of an Andesite and Basaltic Andesite from Western Mexico: Constrains on Water Content and Conditions of Phenocryst Growth," Contrib. Mineral. Petrol. **130**, 304–319 (1998).

30. L. C. Ocala and R. T. Meyer, "Crustal Low Velocity Zone under the Peru–Bolivia Altiplano," Geophys. J. **30**, 199–200 (1972).